AD NUMBER

ADB257455

NEW LIMITATION CHANGE

TO

Approved for public release, distribution unlimited

FROM

Distribution authorized to U.S. Gov't. agencies only; Proprietary Info.; Oct 98. Other requests shall be referred to U.S. Army Medical Research and Materiel Command, 504 Scott St., Fort Detrick, MD 21702-5012.

AUTHORITY

USAMRMC ltr, 27 Feb 2003

AD_____

GRANT NUMBER DAMD17-96-1-6306

TITLE: Genetic and Dyanmic Analysis of Murine Peak Bone Density

PRINCIPAL INVESTIGATOR: Wesley G. Beamer, Ph.D.

CONTRACTING ORGANIZATION: The Jackson Laboratory
Bar Harbor, Maine 04609-1500

REPORT DATE: October 1998

TYPE OF REPORT: Annual

PREPARED FOR: Commander
U.S. Army Medical Research and Materiel Command
Fort Detrick, Frederick, Maryland 21702-5012

NOTICE

USING GOVERNMENT DRAWINGS, SPECIFICATIONS, OR OTHER DATA INCLUDED IN THIS DOCUMENT FOR ANY PURPOSE OTHER THAN GOVERNMENT PROCUREMENT DOES NOT IN ANY WAY OBLIGATE THE U.S. GOVERNMENT. THE FACT THAT THE GOVERNMENT FORMULATED OR SUPPLIED THE DRAWINGS, SPECIFICATIONS, OR OTHER DATA DOES NOT LICENSE THE HOLDER OR ANY OTHER PERSON OR CORPORATION; OR CONVEY ANY RIGHTS OR PERMISSION TO MANUFACTURE, USE, OR SELL ANY PATENTED INVENTION THAT MAY RELATE TO THEM.

LIMITED RIGHTS LEGEND

Award Number: DAMD17-96-1-6306
Organization: The Jackson Laboratory
Location of Limited Rights Data (Pages):

Those portions of the technical data contained in this report marked as limited rights data shall not, without the written permission of the above contractor, be (a) released or disclosed outside the government, (b) used by the Government for manufacture or, in the case of computer software documentation, for preparing the same or similar computer software, or (c) used by a party other than the Government, except that the Government may release or disclose technical data to persons outside the Government, or permit the use of technical data by such persons, if (i) such release, disclosure, or use is necessary for emergency repair or overhaul or (ii) is a release or disclosure of technical data (other than detailed manufacturing or process data) to, or use of such data by, a foreign government that is in the interest of the Government and is required for evaluational or informational purposes, provided in either case that such release, disclosure or use is made subject to a prohibition that the person to whom the data is released or disclosed may not further use, release or disclose such data, and the contractor or subcontractor or subcontractor asserting the restriction is notified of such release, disclosure or use. This legend, together with the indications of the portions of this data which are subject to such limitations, shall be included on any reproduction hereof which includes any part of the portions subject to such limitations.

THIS TECHNICAL REPORT HAS BEEN REVIEWED AND IS APPROVED FOR PUBLICATION.

Patricia C. Maderson 8/7/02

_____ _____

REPORT DOCUMENTATION PAGE

Form Approved
OMB No. 0704-0188

1. AGENCY USE ONLY *(Leave blank)*	2. REPORT DATE	3. REPORT TYPE AND DATES COVERED
	October 1998	Annual (27 Sep 97 - 26 Sep 98)

4. TITLE AND SUBTITLE
Genetic and Dynamic Analysis of Murine Peak Bone Density

5. FUNDING NUMBERS
DAMD17-96-1-6306

6. AUTHOR(S)
Wesley G. Beamer, Ph.D.

7. PERFORMING ORGANIZATION NAME(S) AND ADDRESS(ES)
The Jackson Laboratory
Bar Harbor, Maine 04609-1500

8. PERFORMING ORGANIZATION REPORT NUMBER

9. SPONSORING/MONITORING AGENCY NAME(S) AND ADDRESS(ES)
Commander
U.S. Army Medical Research and Materiel Command
Fort Detrick, Frederick, Maryland 21702-5012

10. SPONSORING/MONITORING AGENCY REPORT NUMBER

11. SUPPLEMENTARY NOTES

12a. DISTRIBUTION / AVAILABILITY STATEMENT

Distribution authorized to U.S. Government agencies only (proprietary information, Oct 98). Other requests for this document shall be referred to U.S. Army Medical Research and Materiel Command, 504 Scott Street, Fort Detrick, Maryland 21702-5012.

12b. DISTRIBUTION CODE

13. ABSTRACT *(Maximum 200*

During the second year of support, the major effort has focused on genetic analyses. We have completed the production of the (C57BL/6 x C3H/He)F2 and (C57BL/6 x CAST/Ei) F2 progenies for analyses of the femoral bone mineral density (BMD) phenotype. We have completed the genotyping of 10% of the populations with highest and lowest BMD from each F2 cross. The genotyping data for B6C3H-F2 mice show significant association of BMD with genetic loci on Chromosomes 1, 4 (two loci), 18, and 13. The genotyping data for B6CAST-F2 mice show significant association of BMD with genetic loci on Chromosomes 1, 3, 5, 13, and 14. In addition, we have tested the 12 BXH recombinant inbred (RI) strains for femoral and lumbar vertebral BMD and compared the resultant strain distribution patterns with polymorphic loci mapped in published data bases. We again found BMD associated with Chrs 1 and 4, supporting the conclusion that these are loci with major effects. Finally, we are developing 10 congenic strains for testing the effect of transferred alleles on BMD. Initial data show that transferred alleles will significantly increase BMD compared with the C57BL/6 as a host strain.

14. SUBJECT TERMS
Osteoporosis, genetics, bone mineral density, bone formation, bone resorption

15. NUMBER OF PAGES
32

16. PRICE CODE

17. SECURITY CLASSIFICATION OF REPORT	18. SECURITY CLASSIFICATION OF THIS PAGE	19. SECURITY CLASSIFICATION OF ABSTRACT	20. LIMITATION OF ABSTRACT
Unclassified	Unclassified	Unclassified	Limited

FOREWORD

Opinions, interpretations, conclusions and recommendations are those of the author and are not necessarily endorsed by the U.S. Army.

____ Where copyrighted material is quoted, permission has been obtained to use such material.

____ Where material from documents designated for limited distribution is quoted, permission has been obtained to use the material.

____ Citations of commercial organizations and trade names in this report do not constitute an official Department of Army endorsement or approval of the products or services of these organizations.

MWB In conducting research using animals, the investigator(s) adhered to the "Guide for the Care and Use of Laboratory Animals," prepared by the Committee on Care and use of Laboratory Animals of the Institute of Laboratory Resources, national Research Council (NIH Publication No. 86-23, Revised 1985).

____ For the protection of human subjects, the investigator(s) adhered to policies of applicable Federal Law 45 CFR 46.

____ In conducting research utilizing recombinant DNA technology, the investigator(s) adhered to current guidelines promulgated by the National Institutes of Health.

____ In the conduct of research utilizing recombinant DNA, the investigator(s) adhered to the NIH Guidelines for Research Involving Recombinant DNA Molecules.

____ In the conduct of research involving hazardous organisms, the investigator(s) adhered to the CDC-NIH Guide for Biosafety in Microbiological and Biomedical Laboratories.

Wesley D. Beamer

PI - Signature Date

TABLE OF CONTENTS

LOMA LINDA UNIVERSITY

School of Medicine
Department of Medicine

Loma Linda, California 92350
FAX: (909) 824-4846

LETTER OF INTENT TO ENTER INTO A CONSORTIUM AGREEMENT

TITLE OF APPLICATION:	Genetic and Dynamic Analyses of Murine Peak Bone Density
APPLICANT ORGANIZATION:	The Jackson Laboratories, Bar Harbor, ME
PRINCIPAL INVESTIGATOR:	Wesley G. Beamer, Ph.D.
COOPERATING INSTITUTION:	Loma Linda University, Loma Linda, CA
PROPOSED PROJECT DATE:	September 27, 1998 through September 26, 1999

The appropriate program and administrative personnel of each institution involved in this grant application are aware of the PHS and National Science Foundation Consortium grant policies and are prepared to establish the necessary inter-institutional agreement consistent with carrying out this project.

Loma Linda University is in compliance with PHS and NSF policies regarding Animal Care and Use, Human Subjects, civil Rights, Handicapped Individuals, Sex Discrimination, Scientific Fraud (Misconduct) Assurance, Delinquent Federal Debt, Debarment and Suspension, Drug-Free Workplace and Lobbying.

Cooperating Institution

By: _____

Date: 10/22/98

David J. Baylink, M.D.
Principal Investigator, LLU
Typed Name and Title

By: _____

Date: 10/23/98

J. Patrick Yhip, C.P.A.
Director, Grants Management, LLU
Typed Name and Title

Applicant Institution

By: Cookie Willems

Date: October 26, 1998

Cookie Willems, CRA
Mgr., Grants Management
Typed Name and Title

By: _____

Date: October 26, 1998

Wesley G. Beamer, Ph.D.
Principal Investigator, TJL
Typed Name and Title

prepared 10/22/98
revised 10/22/98

Year 3 Budget for Army OP Grant (Based on Award)
Budget period: 9/27/98 through 9/26/99

Personnel	Base	Time	Salary	33.00% Fringe	Totals
Postdoctoral Fellow	28,849	100%	28,849	9,520	38,369
Laboratory Tech.	22,214	50%	11,107	3,665	14,773
	Total Personnel		39,956	13,186	53,142
Equipment	Total Equipment				-
Supplies	Histology Supplies		7,761		
	Total Supplies				7,761
Travel	1 national meeting and 1 visit to Jackson Labs				3,423
Other Expense (publications $1,155; and office supplies $525)					1,680
			Subtotal Direct		66,005
			Overhead @ 27%		17,821
			Grant Total		83,827

	Year 1 Award	Year 2 Award	Year 3 Proposed	Year Four	Year Five	Grand Total
Personnel	38,897	50,802	**53,142**	-	-	142,841
Equipment	17,145	-	-	-	-	17,145
Supplies	7,550	7,391	**7,761**	-	-	22,702
Travel	3,260	3,260	**3,423**	-	-	9,943
Other	1,600	1,600	**1,680**	-	-	4,880
Subtotal	68,452	63,053	**66,005**	-	-	197,510
Indirect	13,340	16,394	**17,821**	-	-	46,895
Total	81,792	79,447	**83,827**	-	-	244,405

Indirect Cost Rate: 27%
Based on LLU off-campus and MTDCB, effective July 18, 1998

NOTE: Year 3 budget reflects a 5% increase over year 2 award.
Salaried fringe benefit rate is 33% effective July 18, 1998.

Budget Approved:

David J. Baylink, M.D.
Principal Investigator

J. Patrick Yhip, C.P.A.
Director of Grants Management

ANNUAL REPORT - year 2

5. Introduction

Osteoporosis and the importance of peak bone density

Osteoporosis is a disease of insufficient bone density. In the human skeleton, bone density increases with age, reaching peak levels at 18-22 years of age (1-3). As bone density decreases with age, the risk of osteoporotic fractures increases, especially when the density falls below the fracture threshold. This relationship suggests that the risk of osteoporotic fracture can be defined in terms of two characteristics - the peak bone mineral density (BMD) achieved and the net bone loss rate. The subject of this application is peak BMD, since theoretically, a person with a higher peak BMD would be less likely to fall below the fracture threshold than a person with a lower peak BMD, if both lost bone at a similar rate.

During the past several decades, considerable progress has been made in understanding the pathogenesis of osteoporosis with respect to cellular mechanisms that account for age-related bone loss, but we still know very little about the mechanisms that determine peak BMD. This gap in our understanding has become critical because of recent evidence that as much as 70% of the variation in peak BMD can be accounted for by genetic factors (4). To identify such heritable factors in humans, investigations have primarily focused on unrelated populations to find association of BMD and restriction fragment length polymorphisms (RFLPs) in genes thought to be involved with BMD. One such factor, the vitamin D3 receptor (VDR) has received immense attention with equal numbers of reports showing or not showing a significant relationship between BMD and VDR RFLPs. Other studies have looked for relationships between BMD and serum PTH, collagen, GH levels, and serum mineral. These population studies are subject to sampling bias, lack of knowledge about how many alleles ther are, lack of knowledge about parental sources of genetic alleles, and have low statistical resolving power.

Genetic analysis of peak bone density

Evidence for genetic regulation in humans. In contrast to population association studies, recent studies have disclosed less variation of BMD in young adult monozygotic twin pairs than in dizygotic twins (4, 10, 11). In a study of 71 juvenile and 80 adult male dizygotic and monozygotic twins, Smith et al. found significantly larger variation in radial bone mass and width in dizygotic than in monozygotic twins, indicating the importance of genetic regulation of bone mass (12). In a cross-sectional study of mother-daughter pairs, premenopausal bone density had a strong familial resemblance at the distal forearm, lumbar spine, and proximal femur (13). McKay et al. also reported a strong familial resemblance in lumbar and femoral BMD among mother-daughter and mother-grandmother pairs, although some discordance was noted between the hip and spine sites (14).

Kelly et al. reported a strong genetic effect on serum osteocalcin, a well recognized biochemical marker of bone formation, in both pre- and post-menopausal twins (15). More significantly, within-pair differences in osteocalcin in dizygotic twins predicted within pair differences in bone density at the lumbar spine and femoral neck, suggesting that genetic effects on bone formation relate to bone density. Furthermore, Morrison et al. reported that RFLPs in the VDR gene predicted the variance in serum osteocalcin, whereby both low serum osteocalcin values and the *bb* VDR genotype are associated with a high peak BMD (16).

Difficulties associated with human studies of peak bone density. Genomic diversity and generation time for the human population makes assessment of genes regulating bone density a very difficult undertaking. Twin studies and associative studies with unrelated individuals have substantiated estimates of heritability and provided ways to test relationships between DNA polymorphisms and osteoporosis related traits. However, each approach has its limitations, e.g. relative scarcity of twin pairs, inability to determine number of loci involved, inappropriate evidence to support selected candidate genes, cannot assess interaction between genes and environment, etc. Accompanying the rich genomic heterogeneity of the human population is an equally varied

environment. Although some aspects of environmental variability can be controlled for limited periods of time and others can be assessed by questionnaire, compliance and veracity are always problematic. Long-term studies required to identify critical environmental variables apart from genetic effects are simply not cost effective or practical. Therefore, there is a need for an animal model whose genome and environment can be experimentally manipulated to reveal genes and biochemical mechanisms for acquisition of peak bone density.

Mouse model for genetic analysis of BMD. We have adapted quantitative computerized tomography to develop a genetic model consisting of two inbred strains of mice, C57BL/6J (B6) and C3H/HeJ (C3H), with highly significant differences in peak total BMD in vertebrae (13%), tibia (27%), and femur (53%), with which to identify genes responsible for peak BMD. Preliminary data showed that C3H mice (highest BMD) differed from B6 (lowest BMD) mice as follows: 1) reduced medullary cavity volume and increased cortical thickness; 2) increased metaphyseal trabecular BMD; 3) decreased serum osteocalcin, serum skeletal alkaline phosphatase, and urine crosslinks/creatinine; and 4) decreased osteoclast number at both endosteal cortex and trabecular bone and decreased osteoclast proliferation in marrow cultures at 2 months of age. These morphological and function differences between B6 and C3H mice are genetically founded and strongly suggest that differences in rates for bone formation and resorption account for differences in BMD.

Inbred strain mice, such as B6 and C3H, represent unlimited numbers of genetically identical "twins" whose genes can be experimentally analyzed and whose environments can be strictly controlled. Equally important, each inbred strain is genetically different from every other inbred strain, making possible planned matings and studies of segregating genes. Over the past 10 years, the mouse genome has become highly defined, especially with respect to protein and molecular polymorphic differences among the various inbred strains. This detailed marking of chromosomes greatly facilitates rapid location of new genes. In addition, segments of many chromosomes have been identified that share identical marker loci in mouse and man (17). These homologous segments have provided important clues to mapping human genes associated with a number of diseases including Waardenburg syndrome (18, 19) and retinitis pigmentosa (20). Substantial computerized genetic data bases maintained at The Jackson Laboratory are available to support mapping and biological research efforts that utilize the mouse genome to determine human genetic regulation.

The research proposed in this application focuses on genes that regulate peak BMD in phenotypically normal inbred strains of mice. Because inbred strains exhibit a normal phenotype and an unmanipulated genome, these models of bone regulatory genes are different from murine models that arise from a) spontaneous mutations (osteopetrosis, 26; hypophosphatemia, 27), b) induced mutations resulting from insertion of foreign genes (human *IL-4*; 28), targeted mutated genes (*Mov 13*; 29), or knocked-out genes (*src*-deficient mice; 30).

Quantitative trait loci mapping techniques. Quantitative traits are distinguished from traits with discrete classes (coat color, enzyme deficiency, protein structure variant, or DNA difference that could be detected by Southern blots or PCR) by having a distribution that is more like a bell shaped curve, wherein the extreme ends of the bell shaped curve may predispose to disease. Such traits are determined by many genes and are often influenced by environment. Quantitative traits are the basis for many common diseases: hypertension, atherosclerosis, obesity, type II diabetes, and osteoporosis. Until recently, mapping genes that underlie quantitative traits was not possible, but in the last few years three major advances have come together that now permit geneticists to map the genes underlying quantitative traits.

First, the idea of how to map quantitative trait loci (QTL) was developed by Lander and Botstein (31). The concept is to carry out a cross between two parents that differ in one or more quantitative traits and measure the backcross or F2 intercross progeny for the trait of interest. The extreme ends of the bell shapedphenotype distribution are used for genome analysis. This can be done because the individuals at the extreme high end, for example, will carry all or most of the alleles that cause an individual to be high. Most investigators choose to genotype mice in the upper or lower 5 or 10% of

the phenotype distribution. The entire genome is then scanned by testing for polymorphic markers at intervals of about 15-20 cM. The mouse genome has 1600 cM, so a minimum of 100 markers cover it reasonably well. If the allele that determines the high end of the quantitative trait is designated H and the one determining the low end is called L, then the simplest statistical analysis tests for an excess of H alleles among the individuals at the high end of the distribution and an excess of L alleles at the low end of the distribution.

Second, a major advance is the availability of a large number of molecular markers that are easy to use. During 1995 the Genome Center at MIT completed its task of developing 6000+ polymorphic markers for the mouse (32). These are based on common genetic variations in the length of CA repeats found throughout the mouse genome. The primer pairs are inexpensive ($20/pair) and can be assayed by PCR.

Third, the development is that of computer programs and statistical methods to analyze the large amounts of data. This area is still rapidly evolving. Currently available computer programs are MapMaker (33), QTLCartographer (34-37), and MapManagerQT by Dr. Ken Manly of Roswell Park Memorial Institute, Buffalo, NY. All these programs are available at the Jackson Laboratory and our collaborator, Dr. Frankel, skilled in their use.

Our proposal represents the first attempt to use QTL mapping for the analysis of bone density in B6C3F2 mice. The major problem was not the genetic infrastructure, but the need for reliable methodology for measuring bone density that could be applied to large numbers of mice. This methodological problem has been solved with the peripheral quantitative computerized tomography (XCT 960M) described in Beamer et al (1996). Once major genes have been identified by the first QTL mapping cross (i.e., B6C3F2 mice), further statistical and genetic techniques are able to isolate and study the individual genes. In addition, our new collaborator, Dr. Gary Churchill, Biostatistician, is thoroughly versed in statistical assessment of quantitative data, and is making major contributions and insights to the research product.

6. Body of studies conducted during year 2

Specific Aim 1 (Conducted at The Jackson Laboratory, Bar Harbor, ME). **To map genes that regulate the difference in peak bone density between C3H/HeJ and C57BL/6J mice.** The location of genes responsible for the differences in peak bone density between C3H/HeJ and C57BL/6J strains will be accomplished through combination of genetic crosses and molecular analytical methods:

The genetic crosses utilized in segregating bone density regulatory genes for mapping are: **1)** quantitative trait loci (QTL) analyses of F2 progeny from intercrosses of (C57BL/6J x C3H/HeJ)F1 parents, plus analyses of BXH Recombinant Inbred (RI) strain progeny derived from C57BL/6J and C3H/HeJ progenitors; and, **2)** analyses of Recombinant Congenic (RC) strain progeny derived by backcrossing C3H/HeJ 'donor' genes into the C57BL/6J 'background', plus analyses of progeny from (RC x C57BL/6J)F1 mice backcrossed to the C57BL/6J progenitor strain.

The molecular analytic approaches to assign bone density trait to a specific chromosome are applied to genomic DNA prepared from soft tissues of progeny obtained at necropsy. DNA is scored for molecular markers (simple sequence length and cDNA polymorphisms) that identify genetic alleles originating from either C57BL/6J or C3H/HeJ strains. Co-segregation of molecular markers with bone density phenotypes will establish the genetic linkage to specific chromosomal regions, estimates of the number of genes involved in bone density differences, the location of bone regulatory genes with strong and modifier effects, the mode of inheritance for each gene, the order of the bone density genes with respect to flanking loci, and reveal any parent-of-origin effects on bone density.

Progress

a) Provision of mice for research projects. This year all of the inbred and hybrid mice used in **Aims 1** were raised in Dr. Beamer's animal space at The Jackson Laboratory, Bar Harbor, ME. Colonies of B6, C3H, B6C3F1, and B6C3F2 mice have been the subjects for genetic and endocrinologic analyses carried out in Bar Harbor, ME. Approximately half of the B6 and C3H mice utilized for biochemical and cell biology analyses carried out in Loma Linda, CA, were raised in Dr. Beamer's research colonies, while the remaining half of the mice were purchased from the Animal Resources Colonies of the Jackson Laboratory in Bar Harbor. This collaboration wil continue into all remaining years of the grant period, and it maximizes the efficient use of mice and facilitates co-ordination and interpretation of research results.

b) Phenotypic analyses. Our data indicated that 60-70% of the variance in bone mineral density of B6 and C3H mice is genetically based. Genes responsible for the difference in peak bone density between C3H and B6 mice are being mapped via quantitative trait loci (QTL) analyses of F2 progeny from intercrosses of (C57BL/6J x C3H/HeJ)F1 parents. We have producee 1000 females for phenotypic and genetic analyses. These B6C3H-F2 females have been raised to 4 months of age, then necropsied to obtain serum, body weights, kidneys and skeletal specimens. Femoral bone density has been measured by pQCT (XCT 960M) and shown to be normally distributed curves for both total and cortical bone densities. It is well documented that the B6 and C3H inbred strains differ in at least 50-60% of their respective genomic DNAs. Thus, mapping of chromosomal regions cosegregating with high or low BMD had an excellent chance of success.

An even greater difference in incidence of genomic polymorphism is present between B6 and a wild-derived inbred strain, desginated Castaneus (CAST). Therefore, a parallel mapping study for genes underlying BMD has been carried out with B6CAST-F2 progeny from intercrosses of (B6 x CAST)F1 parents. The objectives of this study were to gain converging lines of evidence regarding loci in B6 that regulate bone density, as well as gain some insight to both additional loci and to existence of allelic variation at loci that might appear in both F2 crosses. We have raised 714 F2 female progeny to 4 months of age, then necropsied these mice, preserving tissues as described for the B6C3H-F2 mice. The distribution of both femoral total and cortical bone densities for both types of F2 females are Gaussian in form, supporting the hypothesis that BMD is a polygenic quantitative trait. Distributions of femoral cortical BMD are presented in **Figure 1**.

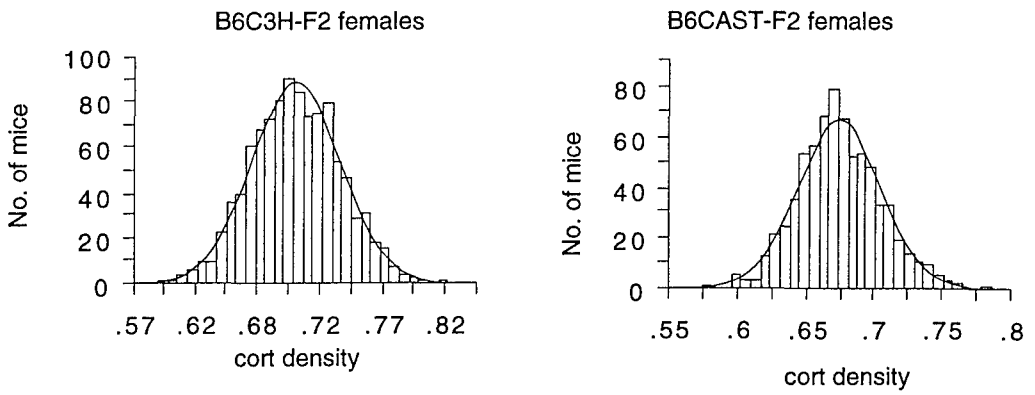

For the purposes of genome-wide survey for loci co-segregating with low or high cortical BMD, we have prepared kidney DNA from approximately 75 mice represented in each extreme tail of the cortical density distribution for each F2 population shown in **Fig 1** (~ 156 B6C3H-F2 and ~145 B6CAST-F2 mice). Genotyping of these mice for polymorphic markers has been accomplished for all 19 autosomes. Genotyping is anticipated to continue for all 1700+ mice for specific markers to define interaction among loci associated with BMD. At this stage, all genetic data are based solely on genotyping for simple sequence length polymorphisms (SSLPs) using PCR methodology that

discriminates B6 from C3H or from CAST alleles at each locus. A total of 110 loci have been typed in 156 B6CH-F2 progeny for all 19 autosomes, and similarly 131 loci in 145 C6CAST-F2 progeny. The objective was typing an average 5 loci/chromosome.

c) Genotype analyses for F2 mapping data. Using MapmanagerQT program, we have found 4 loci in the B6C3H-F2 progeny that meet the (perhaps overly stringent) Lander and Kruglyak (1995) criteria for highly significant linkage with bone density (Chr 4, 1, 18 and 13) and 2 such loci in the B6CAST-F2 progeny (Chr 1 and 5). An additional locus has been identified on Chr 4 of the B6C3H-F2 mice, and 3 additional loci in the B6CAST-F2 progeny (Chr 3, 13, and 14). These data suggest that with the strategic choice of F2 progeny, we have identified 9-10 loci that regulate peak bone density in mice.

With respect to mode of inheritance, thus far alleles at these loci have behaved as additive, with C3H or CAST alleles having strong effects. An exception is Chr 5, where the B6 allele is dominant. Although the markers on Chr 1 are not located at the same chromosomal site, the confidence intervals around the given map positions suggest that only Chr 13 is likely to have different alleles at the same locus. Fine mapping studies are underway to check this issue.

Finally, the most important work on defining gene interaction remains to be done. Statistical assessment of interaction among loci in both crosses has begun in collaboration with Dr. Gary Churchill, The Jackson Laboratory. Additional genotyping (1700 mice x 9 SSLP markers) required for the mathematics is approximately 1/2 completed, thus we cannot yet report on this phase of the genetic analyses.

Table 1. Forward step regressions analyses for loci associated with femoral cortical BMD in F2 mice.

	B6C3H-F2				B6CAST-F2		
Genetic locus	Map dist.	Likeli'd Ratio Stat	Signif. level	Genetic locus	Map dist.	Likeli'd Ratio Stat	Signif. level
D4Mit187	48.1	67.0	2.9×10^{-15}	D1Mit403	99.5	28.3	7.2×10^{-7}
D1Mit282	37.2	40.5	1.6×10^{-9}	D5Mit112	28.4	21.8	1.8×10^{-5}
D18Mit36	15.3	26.9	1.5×10^{-6}	D3Mit23	4.4	16.0	3.4×10^{-4}
D13Mit13	21.9	22.2	1.5×10^{-5}	D13Mit15	3.3	15.4	4.5×10^{-4}
D4Mit226	74.3	16.9	2.2×10^{-4}	D14Mit32	40.4	13.5	1.2×10^{-3}

d) BXH RI strain analyses. The second form of genetic cross proposed for genetic analyses of differences in BMD between B6 and C3H strains incorporated the BXH Recombinant Inbred (RI) strains. This set of 12 inbred strains was derived from intercrosses of (B6 x C3H)F1 parents to produce F2 progeny, then inbreeding individual F2 x F2 sister x brother matings to obtain new strains of mice. At F20, each of these new strains obtained half of its genome from B6 and half from C3H, and each new strain has a different set of genes obtained from each progenitor strain. These BXH RI have been typed for more than 600 polymorphic genes and SSLPs representing all 19 autosomes and the sex chromosomes. In theory, any trait dependent on 1-2 genes that differs between B6 and C3H can be quickly mapped to a chromosome by phenotyping a few mice from each BXH RI strain to obtain the strain distribution pattern (SDP). This pattern is compared to all other SDPs for genes of known chromosomal location.

Virgin BXH RI strain females with mature bone density were necropsied at 8 months to obtain femurs and vertebrae. Femurs were measured for mineral content, volume, high and low density compartments, and linear properties including length, periosteal and endosteal circumferences, and

cortical thickness at the mid-diaphysis. Groups of 6-14 mice for each BXH RI strain were available for this study.

Results - femurs. These data are summarized in **Table 2** below, where the lowest and highest values for each measure are high-lighted for comparison. The B6 and C3H progenitors differed for mineral and total density ($p < 0.001$) phenotypes. When the data for each phenotype were tested for strain differences by one way ANOVA, significant 'p' values (<0.001) were obtained in every case. Furthermore, in every phenotype, we found BXH RI means that were lower, higher, or both than observed in the progenitor strains! Of further import is the fact that femur density was the only phenotype wherein the C3H high density value was not recapitulated in at least one of the BXH RI strains. These data show that the measured 'phenotypes' do not have a genetically simple (1-2 genes) basis, and that there are not enough BXH RI strains for mapping density associated genes.

Table 2. Body weight and femoral parameters from progenitors (C57Bl/6J, C3H/HeJ) and BXH R I strain. Data are X ± SEM (n=6-14 mice/group); Values different from B6 are marked by asterisks.

Strain	Body Weight (g)	Length (mm)	Mineral (mg)	Volume (mm^3)	Total Density (mg/mm^3)
Progenitors					
C57BL/6J	28.2±0.9	16.9±0.18	17.42±0.46	38.00±1.08	0.46±0.009
C3H/HeJ	31.9±3.9	16.6±0.14	24.72±1.66*	36.30±2.22	0.68±0.010*
Recombinant Inbreds					
BXH-2	28.1±1.5	16.3±0.17	**14.00±0.76**	34.12±1.62	**0.41±0.011****
BXH-3	25.6±1.0	16.0±0.11	15.26±0.90	29.64±1.14	0.51±0.013
BXH-4	31.4±1.3	**17.2±0.06**	**27.28±0.32**	**45.60±0.50**	0.60±0.006*
BXH-6	25.7±1.3	16.0±0.05	20.86±0.80	34.50±0.72	0.60±0.012*
BXH-7	26.9±2.3	15.9±0.10	16.60±0.86	31.76±1.16	0.52±0.012
BXH-8	24.3±1.3	16.1±0.11	21.58±1.20	39.16±1.32	0.55±0.016
BXH-9	**31.9±1.9**	16.4±0.05	23.88±0.96	40.78±1.26	0.59±0.007*
BXH-10	26.6±0.7	**15.1±0.07**	15.66±0.24	**28.44±0.48**	0.55±0.004
BXH-11	24.5±1.8	16.4±0.13	21.52±1.06	41.20±1.74	0.52±0.008
BXH-12	28.9±2.5	16.0±0.09	20.60±0.76	34.62±1.04	0.59±0.008*
BXH-14	27.4±1.5	16.5±0.12	23.82±0.76	38.78±0.70	**0.61±0.013***
BXH-19	**21.7±0.4**	16.2±0.07	23.40±0.66	38.72±1.06	0.60±0.008*

To test the conclusion of polygenic basis for the density phenotype, we provisionally assigned each BXH RI a density phenotype as either B6-like or non-B6-like (ie. resembles C3H) via statistical comparison with the B6 progenitor strain. Mean density values similar or lower than B6 were assigned a 'B' phenotype, while means significantly greater than B6 were assigned a 'H' phenotype. The resultant femur density SDP is shown in **Table 3** below, along with the best comparisons to genes with known polymorphisms (B6 vs C3H) found in published data bases. With 12 RI strains, genetic linkage requires the density SDP to be matched with another phenotype in 11 of 12 strains. The best SDP matches that we found were 10 of 12 on Chrs 4, 12, and X. The suggestive linkage to Chr 4 loci is interesting because *Pmv21* (106 cM) is very near the D1Mit403 (99 cM) locus found in the B6C3H-F2 analyses described in Table 1 above. The Chr 12 association was not found in the F2 analyses and is judged spurious. Finally, the Chr X association is the first indication of a X-linked gene for density; this is not testable in the B6C3H-F2 analyses because random X-inactivation in every female cell precludes determining which Chr X allele was active and thus responsible for the

observed phenotype. Further pursuit of the remaining phenotypes of length and body weight are outside the Aims of this application.

Table 3. Comparison of femur densities with strain distribution patterns for known polymorphic loci in BXH RI strains.

		BXH RI Strain												
Locus	B6	C3H2	3	4	6	7	8	9	10	11	12	14	19	Hits
Femur density	B	H	B	B	H	H	B	B	H	B	B	H	H	H	
Chr 1 *Pmv21*	B	H	B	H	H	B	B	B	H	B	B	H	H	H	10/12
Fcgr2	B	H	B	B	B	H	B	B	H	B	B	H	H	B	10/12
Chr 12 *Iap3rc6*	B	H	B	B	H	H	H	B	H	B	B	H	B	H	10/12
Chr X *Pmv6*	B	H	B	B	B	H	B	B	B	B	B	H	H	H	10/12

In summary, the BXH RI strain femur data lead to two conclusions: a) these quantitative phenotypes have a polygenic basis not well suited to a small number of RI's and SDP mapping, and b) phenotypes such as femur size (length, volume) that appear statistically similar in B6 and C3H have different genetic basis that can be segregated in RI strains and also in the B6C3H-F2 progeny (data not shown). Thus, again mapping phenotypes with RI strains whose progenitors do not differ for the phenotype requires alternative genetic matings.

Results - lumbar vertebrae. We also examined individual vertebrae from the BXH RI strains and age matched B6 and C3H progenitors. The L-5 data are presented in **Table 4** below, and reveal that the phenotypes demonstrated greater variation fin the BXH RI strains than observed in the progenitors. As was true for the femur density, the high density of C3H was not achieved in any of the BXH RI strains. Thus, the vertebrae also have a complex genetic basis.

Table 4. Lumbar vertebrae parameters from progenitors (C57Bl/6J, C3H/HeJ) and BXH Recombinant Inbred (RI) strain virgin females that were 8 months of age. (n = 6-14 mice/group)

Strain	Mineral (mg)	Volume (mm^3)	Total density (mg/mm^3)
Progenitors			
C57BL/6J	3.28±0.26	14.08±0.64	0.231±0.010
C3H/HeJ	5.84±0.34*	17.26±0.66*	0.337±0.009*
Recombinant Inbreds			
BXH-2	**1.40±0.116**	**6.52±0.60**	0.216±0.009
BXH-3	2.01±0.22	10.10±1.11	**0.205±0.007***
BXH-4	4.99±0.21	**18.23±0.55**	0.274±0.007
BXH-6	2.86±0.22	12.05±0.76	0.236±0.006
BXH-7	2.78±0.32	12.65±1.20	0.217±0.009
BXH-8	3.73±0.39	15.49±1.35	0.235±0.009
BXH-9	4.55±0.22	17.56±0.70	0.260±0.006*
BXH-10	2.52±0.17	11.25±0.65	0.225±0.007
BXH-11	2.84±0.35	13.32±1.23	0.211±0.006
BXH-12	3.09±0.19	12.73±0.45	0.241±0.007
BXH-14	4.57±0.31	15.00±0.60	**0.303±0.014***
BXH-19	**4.76±0.31**	17.09±0.90	0.278±0.009*

To confirm conclusions derived from the BXH RI femur data described above, a vertebral

density SDP was produced by statistical comparison of RI data with B6 values. Then, either a 'B-like' or 'H-like' phenotype was assigned to each BXH RI strain. The results are presented in **Table 5** below.

Table 5. Comparison of lumbar vertebral densities with strain distribution patterns for known polymorphic loci in BXH recombinant inbred strains.

			BXH RI Strain												
Locus	B6	C3H	2	3	4	6	7	8	9	10	11	12	14	19	Hits
Vert. density	B	H	B	B	H	B	B	B	H	B	B	B	H	H	
Chr 1 *Pmv21*	B	H	B	H	H	B	B	B	H	B	B	H	H	H	10/12
Chr 4 *D4Mit187*	B	H	H	B	H	B	B	B	H	B	B	B	B	H	10/12
Chr 9 *Ets1*	B	H	B	B	H	B	H	B	H	B	B	B	B	H	10/12
Lap1	B	H	B	B	H	B	B	B	H	B	H	B	B	H	10/12

Again, we did not observe the essential 11 of 12 matches between vertebral density and any other polymorphic locus required to establish significant genetic linkage. Nevertheless, Chr 1 *Pmv21* again gave suggestive evidence of linkage as was observed for femoral density in Table 3 above. Also, Chr 4 *D4Mit187* give similar suggestive association with density and this is the best marker that appeared in the B6C3H-F2 analyses reported in Table 1 above. Chr 9 associations were not detected in the B6C3H-F2 analyses and are considered spurious at this time.

In summary, the BXH RI SDP data were not conclusive for loci associated with either femoral or vertebral density. However, associations with the same regions of Chr 1 and 4 were highly significant in the B6C3H-F2 analyses and thus BXH RI data are independent, supportive data for important density regulatory loci. We do not intend to pursue this RI strain analysis for further insights to bone mineral density, primarily because the congenic strains (see below) offer greater power of analyses.

e) Congenic Strains. Analyses of Recombinant Congenic (RC) strain progeny was proposed as a strategy for geneic analyses. It was thought that differences in BMD between strains would only be seen under conditions where several loci could interact. RC strains are derived by two cycles of backcrossing C3H/HeJ 'donor' genes into the C57BL/6J 'background, then sister-brother inbreeding to generate the necessary homozygosity among the two or more loci. In an RC strain, approximately 12.5% of the genes are from the donor strain, while 87.5% are from the recipient. Thus, sets of donor strain genes could be analyzed and mapped as interactive groups of genes.

A simpler and less complex alternative is to prepare congenic strains each of which carries a single chromosomal region-containing a density regulatory locus donated from another strain. Based upon the cortical density loci identified in femur studies summarized in Table 1, we tested the congenic strain methodology by crossing CAST chromosomal regions (Chr 1, 3, 5, 13, and 14) into the B6 strain by 6 cycles of backcrossing (N6). CAST chromosomal segments were followed by flanking polymorphic Mit markers during the backcrossing procedure. Then N6F1 mice were intercrossed to generate N6F2 mice that were genotypically carrying either cast/cast (*c/c*) or b6/b6 (*b/b*) alleles in the relevant genetic segments. These mice are being raised to 4 months of age, then necropsied for tissue and bone specimens. The results for femoral bone density in the first 3 congenics are presented in **Table 6** below.

Table 6. Femoral data for B6.CAST congenic strains at 4 months of age. (n = 12-17 per group)

Strain	Alleles present	Body wt (g)	Length (mm)	Total density (mg/mm^3)	Cortical density (mg/mm^3)
B6.CAST-1	'c/c'	21.8 ± 0.5	15.5 ± 0.1	0.536 ± 0.007***	0.657 ± 0.003**
	'b/b'	21.3 ± 0.6	15.6 ± 0.6	0.496 ± 0.006	0.631 ± 0.004
B6.CAST-3	'c/c'	21.1 ± 0.2	15.2 ± 0.1	0.508 ± 0.005*	0.645 ± 0.004***
	'b/b'	20.8 ± 0.5	15.3 ± 0.1	0.494 ± 0.003	0.625 ± 0.003
B6.CAST-14	'c/c'	19.7 ± 0.3*	15.7 ± 0.1	0.513 ± 0.005**	0.631 ± 0.005*
	'b/b'	21.1 ± 0.4	15.7 ± 0.1	0.486 ± 0.006	0.617 ± 0.004

'p' values: * < 0.05, ** < 0.005, *** < 0.005

We found a modest difference in body weight for B6.CAST-14 mice, and no differences in femur length. Most importantly, we found significant alterations in the total bone and cortical bone density. Therefore, bone density change can result from the introduction of a single CAST chromosomal region containing a density regulatory gene. Thus, the more complex RC strain preparation is not necessary for analyses of single gene effects on bone density. Instead, the simple congenic strain system will allow a) fine genetic mapping leading to cloning of these genes, b) provide virually unlimited numbers of mice to conduct the biological studies that will assist in identifying what these genes do, and c) serve as possible tools for drug discovery aimed at exogenous manipulation of bone density.

There are two more B6.CAST congenics and a total of 5 B6.C3H congenics that will be ready for densitometer assessment within the next 2-6 months. Matings for these congenic strains are being expanded to provide mice to Dr. Baylink and associates in Loma Linda for initial studies of bone formation and resorption.

f) Conclusions. The QTL mapping strategy is work very well and at least 4-5 loci have been found that account for the difference in bone density between B6 and C3H mice, and at least 5 loci account for differences between B6 and CAST/EiJ. Congenic strains either have reached or are nearly ready for measurement of transferred allele effects of BMD, for fine mapping of each locus in preparation for cloning, and for biological studies to determine whether bone formation or bone resorption are the processes most affected by each BMD allele. Determining precisely where thes genes are and what mechanisms they regulate is our overall goal. .

Progress Report of Work Performed at Loma Linda University

This section summarizes the progress of the work performed at Loma Linda University during second year of the funding. To facilitate the understanding of our progress, this section will be subdivided into three sections: In the first section, we will discuss our progress toward the original specific aim (aim 2) of the grant proposal. The second section focuses on progress toward goals that are not included in the original proposal but are relevant to the overall objective of the project. The last section will address what we intend to accomplish during year 3.

I. Progress toward specific aim 2. Our overall objective in this specific aim is to identify bone

modeling (i.e., bone formation and bone resorption) mechanisms that characterize the skeletal phenotypes of C57BL/6J (B6) and C3H/HeJ (C3H) mice. Accordingly, there were two major focuses in our work during the year 2 of this project: 1) to continue measurements of histomorphometric parameters of bone formation and resorption in C57BL/6J, C3H/HeJ and their F1 mice of different age in order to better determine the longitudinal changes in bone formation and resorption that lead to attainment of their respective peak bone density. During the past two years, most of our work has been focused on femur and tibia. However, we have initiated work on measurements of the vertebra. 2) To continue development of biochemical marker assays for mice that are needed for subsequent studies of phenotypic characterization of F1 and F2 mice.

A. ***Longitudinal bone histomorphometric measurements.***

1. Methodology: Before we describe our results thus far, we will briefly summarize the methodology involved. In the progress report for the first year of support, we have already described the methodology that we developed for measurements of diaphyseal histomorphometric parameters. Accordingly, we will herein summarize the methodology that we had developed during the past year for measurements of metaphyseal parameters. Briefly, the distal end of femur (or proximal end of the tibia) were dehydrated in 95% and 100% ethanol, respectively, two days each. After the dehydration, the bone specimens were infiltrated with a mixture containing 85 ml methyl methacrylate, 10 ml glycol methacrylate, 5 ml dibutyryl phthalate, 5 ml polyethylene glycol (PEG 600), and 0.9% dried benzoyl peroxide (as a catalyst) for 4-6 days. Polymerization was initiated by mixing 1 ml of JB-4 solution and 100 ml of the above infiltration solution and was carried out in plastic molding cups (6 x 12 x 5 mm) with the infiltrated specimens placed at the bottom and aluminum blocks placed on top. Each bone specimen was orientated at a position with the anterior part of the femur facing down. To get complete penetration and polymerization, all molding cups were placed in an anaerobic jar and the air removed with vacuum followed by flushing with nitrogen for 5 to 10 min.

Five μm thin bone sections were cut with a Reichert-Jung 1140 Autocut microtome (Buffalo, New York). During sectioning, the knife and tissue blocks were kept wet with 40% ethanol. The resulting sections were either: a) stained with Goldner's for analysis of trabecular bone volume, b) stained histochemically for tartrate-resistant acid phosphatase (TRAP) activity to identify osteoclasts, or c) analyzed unstained for bone formation parameters. All bone histomorphometric parameters were measured with the OsteoMeasureTM system on images captured with a color video camera system equipped with a digitizing tablet (OsteoMetrics, Inc., Atlanta, GA). The sampling site was 0.3 mm down from the growth plate; and the size of the measurement area was between 0.8 to 0.9 mm2. Total tissue area, trabecular bone area, trabecular bone perimeter, tetracycline labeled length, and the width of double tetracycline labels were measured. Trabecular bone volume, thickness, number, mineral apposition rate (MAR), tetracycline labeled surface and total and relative bone formation rate (BFR) were then calculated.

2. Comparison of longitudinal changes in cortical bone formation histomorphometric parameters between C3H and B6 mice.

a. *Bone area.* Consistent with previous pQCT findings, the B6 and C3H mouse strains differ significantly in both tibial cortical and medullary areas. More importantly, the strain-associated differences were detected as early as 6 weeks of age. Accordingly, C3H mice showed a significantly greater cortical bone area than did the B6 mice at all test age ($P<0.001$, ANOVA). Conversely, the medullary area in C3H mice was significantly smaller than that in B6 mice, ranging from 21% smaller ($P=0.004$) at 6 weeks, to 54% smaller ($P<0.001$) at 16 weeks. It should be noted that the total cross-sectional area in C3H mice was not statistically different from that in B6 mice. Therefore, the larger cortical bone area seen in the C3H was primarily due to a smaller medullary cavity area.

Similar to the findings in tibial diaphysis, cortical bone area in femoral diaphysis of C3H mice was also significantly larger than that of B6 mice at all test age. This phenotypic difference can also be detected as early as 6 weeks of age (P=0.002). The femoral medullar area was also significantly smaller in C3H mice than in B6 mice, ranging from 44% at 6 weeks to as much as 70% at 26 weeks of age. However, unlike in tibial diaphysis, the total cross-section area of the femoral diaphysis in C3H mice was significantly less than that in B6 mice at all test ages (P<0.001, ANOVA).

b. *Endosteal bone formation.*

i. Tibia. Table 7 summarizes the longitudinal species-associated differences in the tibial endosteal bone formation parameters. In younger mice, i.e., < 12 weeks of age, the BFR was significantly greater in C3H mice than in B6 mice (P=0.001, ANOVA). Relative BFR (i.e., BFR per bone surface length) was also significantly greater in C3H mice than in B6 mice. However, these species differences in BFR appear to be age-dependent in that in older mice (≥ 16 weeks old), C3H mice exhibited either a similar or reduced BFR (or relative BFR) in comparison to B6 mice of corresponding age. ANOVA confirms a significant strain-related difference in BFR and relative BFR between the two mouse strains. The C3H mice of 16 weeks of age or younger exhibited an elevated MAR (P<0.001, ANOVA), ranging from 51% greater at 6 weeks old (P=0.046) to 94% at 12 weeks (P<0.001), when compared to B6 mice of corresponding ages. However, the MAR of older (i.e., 26 weeks old) C3H mice was lower, albeit not statistically significant, than that of B6 mice. In contrast to MAR, the total label surface (TLS) in C3H mice of all test ages, not only was not higher, but was significantly lower than that in B6 mice. ANOVA also confirms a strain-dependent difference and an age-related changes in both MAR and TLS between the two mouse strain.

That significant differences in bone formation parameters were detected primarily in the younger mice (i.e., 6 to 12 weeks old), supports the possibility that a majority of the strain-related phenotypic changes which lead to differences in bone formation and thus, peak bone mass, may occur during the early age of the animal. We should point out that animals of less than 6 weeks old were not tested in this study. Thus, we do not know whether significant differences in bone mass and BFR can also be detected in animals younger than 6 weeks of age. However, the biggest differences in bone mass and BFR between the two mouse strains were seen with animals of age between 6-12 weeks. Thus, we favor the possibility that larger phenotypic differences concerning bone formation parameters among C3 and B6 mice may occur at ages younger than 6 weeks old. Accordingly, because mice typically undergo puberty at the age between 4 to 5 weeks, we tentatively conclude that the strain-dependent phenotypic differences between the two mouse strains most likely occur during the time of their puberty. If this conclusion is confirmed, it can be speculated that the gene(s) which contribute to the differences in bone formation rate and in peak bone mass in these mice are expressed predominantly during puberty. This information is very important in relation to our continuing efforts of searching for genes that are involved in peak bone mass determination because if this conclusion is valid, it would be essential for us to use animals during puberty to search for genes that regulate peak bone mass.

Table 7. Tibial endosteal bone formation histomorphometric parameters of C3H and B6 mice.

Age/Strain	BFR (mm3 x 10-3/day)	Relative BFR (mm3x10-3/mm2/day)	MAR (μm/day)	Total label surface (mm2)
6 weeks				
C3H	3.012±0.417	1.656±0.184*	2.574±0.334*	1.165±0.035
B6	2.161±0.292	1.054±0.133	1.703±0.171	1.263±0.105
8 weeks				
C3H	3.077±0.260	1.944±0.149*	2.475±0.140***	1.226±0.041***
B6	2.848±0.096	1.386±0.046	1.604±0.046	1.779±0.042
12 weeks				
C3H	2.445±0.115**	1.659±0.066***	2.155±0.110***	1.144±0.041*
B6	1.485±0.056	0.764±0.039	1.108±0.038	1.362±0.076
16 weeks				
C3H	1.385±0.114	1.013±0.082*	1.136±0.043*	1.210±0.066*
B6	1.485±0.056	0.729±0.067	0.968±0.056	1.499±0.076
26 weeks				
C3H	0.617±0.086***	0.428±0.057***	0.878±0.098	0.698±0.041***
B6	1.792±0.123	0.963±0.073	1.154±0.075	1.557±0.058
P valuey				
Strain	0.001	<0.001	<0.001	<0.001
Age	<0.001	0.009	<0.001	<0.001
Strain x Age	NS	NS	NS	0.003

*P<0.05 vs. B6; **P<0.01 vs. B6; ***P<0.001 vs. B6; NS = not significant; y6-12 weeks old.

The finding that the strain-related increase in BFR in C3H mice appeared to be associated with a higher MAR without a significant increase in TLS compared to B6 mice is intriguing. In this respect, BFR is determined by two major parameters: a) the number of active osteoblasts, and b) the activity of osteoblasts. Histomorphometrically, BFR is calculated by multiplying MAR by TLS. Accordingly, since it is generally assumed that TLS is an index of the number of active osteoblasts that line up on bone forming sites, it follows that MAR may be regarded as an acceptable indicator of the bone forming activity of osteoblasts. That, there is a strain-associated elevation in MAR but not TLS in C3 mice compared to B6 mice, raises an interesting possibility that the greater peak bone mass in C3 mice (as opposed to B6 mice) may be related to at least in part an increase in bone formation rate that is due exclusively to an increase in the activity, but not the recruitment (proliferation), of osteoblasts. While this conclusion needs to be confirmed by additional work, this is exciting because this represents strong histomorphometric evidence that bone formation can be increased through an activation of existing osteoblasts without a stimulation of osteoblast proliferation. This concept is entirely consistent with the conclusion of Charles Turner and colleagues that PTH treatment stimulates bone formation through activation of lining cells (inactive osteoblasts) without a stimulation of osteoblast proliferation. In further support of the premise that MAR is an important parameter of bone mass, it was shown, in the mouse senescence model, SAM-P/2, SAM-P1, and SAM-P6 mice, that a higher endosteal MAR was associated with a greater bone mass. These findings may have an important implication with respect to our efforts of searching for gene(s) that control peak bone mass if our conclusion that osteoblast activity (i.e., MAR) plays a more essential role than osteoblast proliferation (i.e., TLS) in determining the peak bone mass in these mice is confirmed. Accordingly, it may be speculated that the genes that help to determine peak bone mass in these mice may be those which are involved in regulating osteoblast differentiation and/or activity.

ii. *Femur*. Table 8 shows the bone formation histomorphometric parameters in femur of C3H and B6 mice. Unlike tibial endosteal BFR, there was no significant strain-dependent difference in femoral endosteal BFR from 6 to 12 weeks. However, the femoral endosteal relative BFR in the young C3H vs. B6 mice, similar to the tibial endosteal BFR, was significantly (P<0.001, ANOVA) higher. In the older mice (i.e., >12 weeks old), the femoral endosteal BFR was significantly less in C3H mice than in B6 mice. Similar decreases in relative BFR were observed in the femoral endosteum in older C3H mice compared to that in B6 mice with the same age (P<0.001). Two-way ANOVA indicates while there appears to be an age effect on BFR and a strain and an age effect on relative BFR, there was no significant interaction between age and strain on either BFR or relative BFR.

Table 8. Femoral endosteal bone formation histomorphometric parameters of C3H and B6 mice.

Age/Strain	BFR (mm3 x 10-3/day)	Relative BFR (mm3x10-3/mm2/day)	MAR (μm/day)	Total label surface (mm2)
6 weeks				
C3H	18.48±0.42	5.945±0.142	6.010±0.165	3.080±0.055***
B6	19.45±2.29	4.643±0.527	4.808±0.546	4.050±0.122
8 weeks				
C3H	11.04±0.59	3.967±0.210**	4.367±0.190**	2.525±0.081
B6	8.37±2.00	2.071±0.461	2.597±0.406	3.002±0.331
12 weeks				
C3H	5.518±0.332	2.220±0.098***	2.749±0.113***	2.015±0.110***
B6	5.652±0.487	1.467±0.128	1.773±0.109	3.161±0.108
16 weeks				
C3H	2.258±0.247**	0.975±0.104	1.294±0.0.079	1.714±0.104***
B6	3.847±0.416	1.002±0.107	1.336±0.109	2.835±0.134
26 weeks				
C3H	0.585±0.056***	0.296±0.031***	0.788±0.075*	0.768±0.059***
B6	2.561±0.275	0.714±0.071	1.022±0.076	2.473±0.114
P valuey				
Strain	NS	<0.001	<0.001	<0.001
Age	<0.001	<0.001	<0.001	<0.001
Strain x Age	NS	NS	NS	NS

*P<0.05 vs. B6; **P<0.01 vs. B6; ***P<0.001 vs. B6; NS = not significant; y6-12 weeks old.

As in the tibia, the femur in C3H mice of 6-12 weeks old showed a significantly (P<0.001) greater endosteal MAR than the femur in B6 mice of corresponding age. Also, as in tibia, the older C3H mice (i.e., 26 weeks old) also showed a significantly lower endosteal MAR than B6 mice. The femur, similar to tibia, also has a smaller (P<0.001) endosteal TLS in C3 mice of all test age than B6 mice: 24% smaller at 6 weeks (P<0.001), 36% smaller at 12 weeks (P<0.001), 40% smaller at 16 weeks, and 69% smaller at 26 weeks (P<0.001), respectively. Two-way ANOVA also shows no significant interaction between age and strain on either MAR or TLS.

These observations indicate that the strain difference in endosteal bone formation parameters are similar in both tibia and in femur, suggesting that these strain-related phenotypic differences in endosteal bone formation parameters between the two mouse strains may be general throughout the skeleton and not bone site specific. We should note that, while we have initiated measurements on

bone formation histomorphometric parameters in vertebra, we have not yet completed the analysis. Accordingly, we do not know as of now whether these strain-associated differences in bone formation parameters are maintained in vertebrae.

c. *Periosteal bone formation.*

i. *Tibia*. Table 9 shows the tibial periosteal bone formation histomorphometric parameters of the two mouse strains. Interestingly, periosteal BFR in young C3H mice was also significantly (P<0.001, ANOVA) greater than that in young B6 mice, ranging from 29% at 6 weeks to 290% at 12 weeks. Relative BFR was also significantly greater in C3H mice than B6 mice from 6 to 12 weeks (P<0.001, ANOVA).

Table 9. Tibial periosteal bone formation histomorphometric parameters of C3H and B6 mice.

Age/Strain	BFR (mm3 x 10-3/day)	Relative BFR (mm3x10-3/mm2/day)	MAR (μm/day)	Total label surface (mm2)
6 weeks				
C3H	8.538±0.365*	2.596±0.125*	3.212±0.142**	2.675±0.126
B6	6.609±0.612	2.063±0.189	2.394±0.193	2.748±0.058
8 weeks				
C3H	5.873±0.337***	1.807±0.106***	2.741±0.066***	2.143±0.114
B6	3.049±0.346	0.923±0.105	1.677±0.079	1.823±0.204
12 weeks				
C3H	3.989±0.236***	1.175±0.062***	2.172±0.134***	1.841±0.036***
B6	1.024±0.143	0.310±0.045	0.926±0.041	1.079±0.124
16 weeks				
C3H	1.463±0.034	0.438±0.010	0.811±0.027	1.813±0.060**
B6	1.215±0.296	0.356±0.086	0.921±0.115	1.130±0.188
26 weeks				
C3H	1.172±0.125	0.338±0.036	0.708±0.034	1.630±0.133
B6	0.985±0.088	0.291±0.027	0.704±0.037	1.386±0.054
P valuey				
Strain	0.001	<0.001	<0.001	0.003
Age	<0.001	<0.001	<0.001	<0.001
Strain x Age	NS	NS	NS	0.013

*P<0.05 vs. B6; **P<0.01 vs. B6; ***P<0.001 vs. B6; NS = not significant; y6-12 weeks old.

The periosteal MAR in tibia was also significantly (P<0.001, ANOVA) larger in C3H mice than that in B6 mice from 6 to 12 weeks old. Similar to the endosteal tibial MAR, the periosteal MAR in tibia was also no longer different between the two strains at the later ages (16 weeks and 26 weeks old). While there was no statistically significant difference in TLS at the periosteum of tibia between the two mouse strains at most of the test age, the TLS in 12 and 16 weeks old C3H mice, respectively, was significantly greater than that in B6 of corresponding age. Accordingly, one may speculate that unlike endosteal bone formation, changes in both osteoblast activity and number may play a role in the strain-dependent difference in tibia periosteal bone formation between the two mouse strains.

We must emphasize, however, that the cross-section area of the tibia between the two mouse strains was not significantly different. Thus, it is interesting that tibial periosteal BFR in C3H mice is greater than that in B6 mice. In order for the two mouse strains not to differ in cross-section area in

tibia, it can be speculated that the tibial periosteal bone resorption rate in C3H mice must also be greater (presumably at the same magnitude as that of BFR) than that in B6. We are currently testing this possibility by investigating periosteal bone resorption parameters.

ii. *Femur*. Table 10 reveals that the strain-associated longitudinal changes in femoral periosteal bone formation parameters were very similar to those in tibial periosteal bone formation parameters. Periosteal BFR in femur of the young C3H mice was also larger than that of B6 mice. Similarly, the relative BFR is also larger in C3H mice than B6 mice ($P<0.001$, ANOVA). Interestingly, unlike tibial periosteum but similar to tibial endosteum, the periosteal MAR in femur was also significantly higher ($P<0.001$, ANOVA) in C3H mice of age from 6-12 weeks, without a significant difference in TLS.

Table 10. Femoral periosteal bone formation histomorphometric parameters of C3H and B6 mice.

Age/Strain	BFR (mm3 x 10-3/day)	Relative BFR (mm3x10-3/mm2/day)	MAR (μm/day)	Total label surface (mm2)
6 weeks				
C3H	5.151±0.604***	1.201±0.145**	2.176±0.230*	2.346±0.072
B6	2.668±0.446	0.272±0.095	1.277±0.179	2.090±0.137
8 weeks				
C3H	5.829±0.364	1.380±0.087	2.472±0.159	2.385±0.112***
B6	6.246±1.155	1.269±0.245	1.948±0.300	3.128±0.112
12 weeks				
C3H	4.071±0.241***	0.934±0.056***	1.697±0.077***	2.398±0.076
B6	2.392±0.239	0.483±0.048	1.156±0.051	2.077±0.212
16 weeks				
C3H	3.001±0.229**	0.689±0.055**	1.383±0.090**	2.170±0.063*
B6	1.902±0.124	0.394±0.025	1.000±0.069	1.902±0.062
26 weeks				
C3H	2.509±0.174*	0.550±0.037*	1.038±0.050	2.428±0.148*
B6	1.548±0.322	0.319±0.065	0.903±0.081	1.631±0.221
P valuey				
Strain	<0.001	<0.001	<0.001	NS
Age	<0.001	<0.001	0.003	0.001
Strain x Age	NS	NS	NS	0.001

*P<0.05 vs. B6; **P<0.01 vs. B6; ***P<0.001 vs. B6; NS = not significant; y6-12 weeks old.

In summary, we have evidence that differences in BFR and/or MAR are detected at both periosteal as well as endosteal bone sites. The differences in bone area and BFR are also evident at tibia as well femur. Consequently, these observations are entirely consistent with the contention that the strain-associated difference in bone formation and bone mass is not site-specific. These findings are consistent with our previous observations that the strain-related difference in bone density was evident in the vertebra, proximal phalanges, tibia, as well as femur.

3. Comparison of trabecular bone formation histomorphometric parameters between C3H and B6 mice.

a. *Trabecular bone volume*. We found that C3H mice also had a significantly greater trabecular bone volume than B6 mice: 32% greater at 6 weeks old and 64% at 12 weeks old. While trabecular bone volume appeared to decline with age in both mouse strains, the effects of strain ($P=0.040$) and

age (P=0.002) were highly significant. However, the larger trabecular bone volume seen in C3H mice was not a result of a larger number of trabeculae (since there was no significant difference in the number of trabeculae between the two mouse strains at both 6- and 12-week old. Rather, it was due to a larger trabecular thickness since C3H mice had a 16% and 49% larger trabecular thickness at 6 weeks and 12 weeks old, respectively.

b. *Trabecular bone formation parameters.* Comparison of bone formation parameters of trabeculae between C3H and B6 mice of 6 and 12 weeks old, respectively. BFR rate in trabeculae in C3H, like in cortical bone, was significantly (P=0.006, ANOVA) higher than that in B6 mice of 6 week (23%) or 12 week (68%) of age. Correspondingly, MAR was also 29% and 23% higher (P=0.001, ANOVA) in C3H mice of 6 and 12 weeks old, respectively, than in B6 mice of corresponding age. Conversely, TLS in trabeculae was not significantly different in either strains of either age. These findings suggest that, like in cortical bone, C3H mice has a higher BFR in trabecular bone than B6 mice, and that the increased trabecular bone formation appeared to be caused by an increased osteoblast activity rather than an increased osteoblast proliferation.

c. *Trabecular bone resorption parameters.* Inasmuch there is strong evidence that a major contributor to different peak bone mass between C3H and B6 mice is difference in bone formation capability in the two mouse strains, we cannot rule out the possibility that differences in bone resorption parameters may also contribute to the observed strain-associated difference in peak bone mass. This possibility is supported by our recently completed in vitro study which shows that C3H mice also have a lower bone resorptive capability, i.e., lower ability to produce mature osteoclasts *in vitro*. This work has recently been accepted for publication in Journal of Bone and Mineral Research (Linkhart et al., Osteoclast formation in bone marrow cultures from two inbred strains of mice with different bone densities. J. Bone Miner Res in press). Thus, we will not include these in vitro findings in this progress report. We sought to confirm this in vitro observation in mice. Accordingly, we performed a histomorphometric study to determine the number of osteoclasts in secondary spongiosa of distal femur of 5.5 week-old female B6 and C3H mice. The results are shown in Table 11.

Table 11. Osteoclast numbers in secondary spongiosa of distal femur of 5.5 week-old female B6 and C3H mice. The sample area was from 0.3 to 0.78 mm proximal to the distal growth plate cartilage. Data are shown as mean±SEM. Significant differences between mouse strains were tested by one-way ANOVA.

Parameters	**B6 (n=7)**	**C3H (n=6)**	**P value**
Total area (mm2)	0.889±0.031	0.826±0.026	NS
Osteoclasts per mm2 total area	249±13	103±18	<0.001
Bone surface (mm)	14.7±1.6	11.4±1.4	N.S.
Osteoclasts per mm bone surface	15.6±1.0	7.5±1.0	<0.001
Osteoclast surface/bone surface	0.348±0.028	0.171±0.016	<0.001

This study indicates that C3H mice contain significantly less: 1) osteoclasts per total bone area, 2) osteoclasts per bone surface, and 3) osteoclast surface/bone surface when compared to B6 mice. We next tested whether C3H has a lower bone resorption surface than B6; we measured the total resorbing surface on bone sections of femoral metaphysis of 6 week old C3H and B6 mice. Figure 5 illustrates that C3H mice indeed had a 53% less resorbing surface on trabecular bone than B6 mice. Thus, these observations are consistent with the in vitro findings that C3H bone contains less osteoclast precursors and less ability for osteoclastogenesis. Accordingly, this supports the likely possibility that the higher peak bone mass in C3H mice may be due to, in addition to an increased

BFR, a reduced bone resorption rate. We are currently investigating this possibility. If this is confirmed, it would mean that genes responsible for peak bone mass would be comprised of genes regulating both bone formation as well as bone resorption.

4. Comparison of bone histomorphometric parameters among B6, C3H, and their F1 hybrid. We have now begun studies involving the F1 mice. Figure 6 summarizes the total cross-section area, medullary cavity, and cortical bone area of tibia in F1 compared to those in their parent strains at age 12 weeks and 16 weeks old. Again, there was no significant difference in total tibial cross-section area among B6, C3H, and F1 mice. B6 mice had bigger medullary cavity than C3H. While the medullary cavity of F1 cross was smaller than that of B6, it was greater than C3H (i.e., an intermediate medullary cavity). Similarly, the cortical bone area of the F1 mice was also fell between that of C3H and B6. This was true at both ages.

Histomorphometric bone formation parameters at the endosteum in F1 and the parent strains were also compared. The values of BFR, MAR and TLS of F1 at 12 weeks of age, like the cortical bone area, lay between those of the parent strains. Very interestingly, at 16 weeks of age, with the exception of MAR, both BFR and TLS of F1 mice were significantly lower than those of both C3H and B6 mice. This is very intriguing, and we do not yet have an explanation for these observations. On the other hand, we observed that periosteal MAR, TLS, and BFR values in the tibia of F1 mice, similar to cortical bone volume, were found to be somewhere between those values of C3H (which had high values) and those of B6 (low values). However, the MAR and BFR of the F1 mice were more closely to those of the B6 mice than to those of the C3H mice. Nevertheless, these findings are consistent with the predicted phenotype changes in F1 progenies.

B. ***Development of murine biochemical marker assays of bone turnover.*** Murine biochemical markers of bone formation and resorption are essential for rapid phenotypic characterization of bone turnover in parent strains and F1 and F2 progenies. Unfortunately, there is no readily available markers assay for mouse. Accordingly, a major specific aim of this project was to develop murine biochemical marker assays of bone turnover. Once these assays are validated and available for routine use, we will apply these assays to phenotypically characterize our mouse strains and their progenies.

In the previous progress report, we have already summarized our progress in several bone formation and resorption marker assays, i.e., osteocalcin, alkaline phosphatase, osteoclastic TRAP, and several growth factor assays as well as mouse creatinine assay. In this report, we will summarize our progress in development of a urine-based bone resorption assay, namely, urinary pyridinoline and deoxypyridinoline crosslinks assays.

The total pyridinoline (PYR) and deoxypyridinoline (DPYR) in urine were analyzed by a high-pressure liquid chromatography (HPLC) approach. The crosslinks were first hydrolyzed with 6N HCl to release protein bound PYR and DPYR. The released PYR and DPYR were then partially purified by partition chromatogrphy and concentrated prior to quantitation on HPLC, using a reverse phase C18 column. The crosslinks are eluted with a gradient of heptafluorobutric acid (an ion pairing agent) and acetonitrile. The crosslinks were detected by fluorescence emission using an excitation wavelength of 295 nm and an emission wavelength of 395 nm. Acetylated-PYR (ACP) was added in each run as an internal standard and the method was quantitated using an external standard curve of known amounts of PYR and DPYR, respectively. The averaged intra-assay and inter-assay variation for the measurement of PYR and DPYR was <12% for each.

To validate the assay, 24-hour urine sample from C3H and B6 mice were obtained. Concentrations

of PYR and DPYR crosslinks were determined and standardized against urinary creatinine (CRT) concentration to account for differences in urine volume. Table 12 compares the urinary levels of PYR and DPYR between C3H and B6 mice at 2 months and 8 months old.

Table 12. Urinary levels of PYR and DPYR in C3H and B6 mice. Results are shown as mean±SD (number of mice).

Age	PYR in B6 (nmol/mmol CRT)	PYR in C3H (nmol/mmol CRT)	P-value (Mann-whitney)	DPYR in B6 (nmol/mmol CRT)	DPYR in C3H (nmol/mmol CRT)	P-value (Mann-whitney)
2 months	163.6±52.8 (10)	119.37±17.1 (9)	0.1128	20.57±6.87 (10)	15.01±6.42 (9)	0.0789
8 months	107.3±29.4 (8)	100.6±11.96 (9)	0.9654	15.23±4.00 (8)	14.54±4.70 (9)	0.6965

These data indicates that urine PYR/CRT and DPYR/CRT measured by our HPLC methods appeared to be higher in B6 mice compared to C3H, especially in the younger mice (2 months old). Unfortunately, the differences were not statistically significant. One of the possible reasons for the non-significance may be related to the relatively large assay variations. On the other hand, our bone histomorphometric studies suggest that strain-associated differences in bone turnover rates that lead to differences in peak bone mass occurred at earlier age. An alternative explanation may be due to the fact that much older mice were used in this study. Nevertheless, that, the urine crosslinks levels in B6 mice appeared to be higher than those in C3H mice, is consistent with our findings that C3H mice exhibited a lower bone resorption rate than B6 mice. We are currently working on improving the variation of the assay and on further validating this assay.

II. Progress toward goals that are not in the original specific aims but are relevant to the overall objective of the project. During the course of the study, we became interested in the hypothesis that the differences in peak bone mass seen in the two mouse strains may also be caused by a difference in their bone responses to bone remodeling stimuli. In other words, the higher BFR seen in C3H mice could be caused by a hypersensitivity of osteoblasts in this mouse strain to bone formation stimuli, such as mechanical loading, or the lower BFR seen in B6 mice is the result of inability of osteoblasts in this mouse strain to respond to bone formation stimuli. Conversely, the lower bone resorption observed in C3H mice might be due to the inability of their osteoclasts to respond to bone resorption stimuli.

To test this hypothesis, we have performed two sets of experiments in these two mouse strains to determine whether these two mouse strains would respond differently to bone formation stimuli (or the lack of) and bone resorption stimuli, respectively. Accordingly, mechanical loading is a well-known bone formation stimulus. Therefore, we wanted to assess the role of responsiveness to mechanical loading as a possible determinant of the bone density difference between C3H and B6 mice. We reasoned that, if osteoblasts of these two mouse strains indeed exhibit different responses to bone formation stimuli, the removal of mechanical loading by sciatic neurectomy should produce different responses on bone formation or resorption parameters in these two mouse strains. Therefore, in the first study we examined and compared the effects of sciatic neurectomy on bone formation parameters of tibia in C3H and B6 mice. Conversely, calcium deficient animals develop secondary hyperparathyroidism, which is a potent stimulus of osteoclastic resorption. Consequently, in the second study, we determined and compared the effects of calcium deficiency on tibial bone resorption parameters in these two mouse strains.

A. ***Sciatic neurectomy***. In the preliminary study, sciatic neurectomy was performed on the left legs of seven C3H and eight B6 mice of 8 weeks of age. The right legs of each animal served as a control. During the following week, we noted some of the mice chewing on their immobilized limbs. To prevent this behavior, we wrapped the neurectomized legs in cotton gauze and several layers of duct tape affixing the immobilized leg to the tail in the process. This reduced the incidence of chewing and prevented self-mutilation. After 3 weeks of immobilization, the mice were euthanized and the tibiae dissected for histomorphometric analysis of bone formation parameters in cortical bone.

Table 13 summarizes the results of this preliminary experiment. This preliminary study of sciatic neurectomy in C3H and B6 mice showed a greater medullary area, at the tibial-fibular junction, in B6 mice, compared to C3H mice, but no effects of neurectomy. Although the procedure was effective (i.e., the hindlimb was immobilized), the immobilization was without apparent effect (i.e., the -25% measured difference in medullary area in the B6 neurectomized leg, compared to the contralateral control, was not statistically significant).

Table 13. Effects of sciatic neurectomy (21 days) on cross-sectional areas at the tibial-fibular junction in C3H and B6 mice. (Results are expressed as mean±SEM).

		Cross-sectional area (mm2)	
Mouse strain	Treatment (n)	Total area	Medullary area
C3H	Control (8)	0.930±0.025	0.120±0.007
	Neurectomy (8)	0.959±0.039	0.125±0.009
B6 (7)	Control (7)	0.871±0.016	0.259±0.016*
	Neurectomy (7)	0.911±0.035	0.325±0.032*

*Indicates a significant difference, compared to C3H mice, $p<0.001$. There were no significant effects of the sciatic neurectomy on either cross-sectional area.

Reasoning that a time-dependent effect might become more evident with a longer post-operative period and that a greater number of mice in each group would increase the power to detect a significant difference, we subsequently performed a longer study, with an increased number of mice in each group. We also amended the study design to include sham-operated mice as an additional control for the immobilized legs. We anticipated that these additional control groups would allow us to test the potentially confounding hypothesis that immobilization of one leg could result in overloading of the contralateral leg and, thereby, distort that comparison. Accordingly, 30 seven-week old mice of each strain, after 2 weeks of acclimation, were randomly divided into three groups of ten, for each strain: a baseline control group to be euthanized on day 0; a sham-operated control group; and a sciatic neurectomized group. The mice were ~9 weeks of age at the start of the study. After the operation, cotton gauze and duct tape were used to immobilize the neurectomized left leg as described above. No duct tape was applied to the sham operated group. The experiment was carried out for 28 days. All animal were euthanized, blood was collected from each animal for measurements of serum bone formation markers, i.e., alkaline phosphatase (ALP) and osteocalcin (OC). The tibiae from both legs of each mouse were removed for bone histomorphometric measurements. The femora were extracted for 72 hours at 4oC with 1.5 ml of 25 mM NaHCO3 (pH 7.4) containing 0.01% azide and 0.01% Triton X-100. ALP and OC contents in each extract were determined. The extracted bones were dehydrated with 1 ml 70% ethanol followed by drying at 37oC and measurement of dry bone weight.

Table 14 summarizes the results of the second study, with respect to body weight and two serum indices of bone formation: ALP and OC. Although the body weights of both strains of mice were increased during the study (i.e., from 9 to 13 weeks of age), there were no significant differences in

final body weight between the neurectomized and sham-control mice or between the C3H and B6 mice in either group. Similarly, we noted significant decreases in serum ALP activity, between 9 and 13 weeks of age, in both strains of mouse, but again, no effects of neurectomy. The only significant change in serum osteocalcin was a decrease in the B6 sham group, compared to the basal controls. Thus, these data demonstrate that four weeks of hindlimb immobilization, following sciatic neurectomy, did not produce changes in body weight, serum ALP, or serum OC.

Table 14. Effects of 4 weeks sciatic neurectomy on body weight and serum bone formation markers in C3H and B6 mice.

Strain - treatment (n)	Final body weight (g)	Weight gain (g)	Serum ALP (mU/ml)	Serum OC (ng/ml)
C3H Basal (10)	18.5±0.4	--------	195±6	35.6±4.8
Sham (8)	20.4±0.6*	2.4±0.3	147±8#	34.5±5.0
Neurec (10)	19.7±0.2*	3.0±0.2	166±8*	22.1±4.1
B6 Basal (10)	18.3±0.2	--------	208±10	54.8±6.6
Sham (8)	21.1±0.3#	3.0±0.2	148±4#	29.0±3.3#
Neurec (10)	20.5±0.2#	2.5±0.3	162±11#	37.8±3.7

All data shown as mean±SEM. *Different from the basal control group of the same strain, P<0.05; #P<0.005. There were no significant differences (ANOVA) between the group of C3H and B6 mice that received the same treatment (i.e., basal, sham, or neurectomized). There were no significant differences between the neurectomized and sham control groups of either strain (i.e., no effects of neurectomy).

Bone extraction studies (Table 15) revealed significant differences in femur dry weight, ALP/mg bone, and OC/mg bone, between the 9 week-old basal control groups and the 13 week-old sham and neurectomized groups of each strain. In addition, measurements of femur dry weight showed the anticipated differences between the bones of C3H and B6 mice, in every treatment group, but no effects of neurectomy. There were no differences in ALP activity/mg dry weight of bone between the C3H and B6 mice or between the neurectomized and sham-operated mice of either strain. There were, however, differences in extractable OC (expressed as ng/mg dry weight), between the C3H and B6 mice at 13 weeks of age. We found no effects of neurectomy on femur dry weight, ALP activity/mg dry weight, or extractable OC/mg dry weight.

Table 15. Effects of sciatic neurectomy (4 weeks) on femoral extract ALP and OC contents.

	Right (Control) Femur			**Left (Neurectomized) Femur**		
Strain – treatment	Dry weight (mg)	ALP (mU/mg)	OC (ng/mg)	Dry weight (mg)	ALP (mU/mg)	OC (ng/mg)
C3H						
Basal	34.6±1.6	15.6±1.5	0.20±0.02	35.0±0.9	21.3±1.1	0.14±0.02
Sham	43.9±1.1#	7.1±0.6#	0.28±0.05	43.1±1.2#	8.0±0.8#	0.33±0.06#
Neurect.	44.8±0.8#	5.4±0.3#	0.24±0.03^	43.4±0.9#	6.3±0.5#	0.34±0.05#
B6						
Basal	30.2±1.6	18.5±1.6	0.23±0.05	28.0±2.0&	21.8±2.9	0.20±0.03
Sham	36.5±0.5* &	9.2±0.8#	0.18±0.02	35.5±1.1# &	9.5±0.8#	0.20±0.03
Neurect.	35.8±1.2* &	7.2±0.6#	0.12±0.02	34.3±1.5# &	8.7±0.8#	0.16±0.02 &

*Different from the same-leg basal control group of the same strain, P<0.05; #P<0.005. ^Different from the same-leg (i.e., left or right) of the C3H mice receiving the same treatment, P<0.05,

&P<0.005. There were no significant differences between the neurectomized legs and the contralateral controls or between the neurectomized legs and the sham-operated control legs of either strain (i.e., no effects of neurectomy).

Histomorphometric measurements of ground sections at the tibial-fibular junction confirmed that the 9-week-old basal control mice had similar total bone areas (0.829±0.012 mm2 for C3H mice, compared to 0.827±0.018 mm2 for B6 mice), but differed greatly, with respect to medullary area. Medullary area in the B6 mice (0.341±0.017 mm2) was ~90% greater than in the C3H mice (0.176±0.005 mm2, P<0.001). Table 10 showed that medullary area at the tibial-fibular junction was increased by neurectomy, in B6 mice, compared to the contralateral controls. The difference was also significant, compared to the sham controls. In contrast to these results, we found no significant difference in any measured parameter the left and right tibiae of the sham controls of either strain. Assessments of endosteal resorbing surface showed neurectomy-dependent increases in both strains of mice. Endosteal resorbing surface was increased in the neurectomized legs of C3H, compared to both the contralateral and sham-operated controls and this effect of neurectomy was even more pronounced in B6 mice. Further histomorphometric assessments at the tibial-fibular junction also revealed that endosteal bone forming surface was dramatically decreased by neurectomy in B6 mice, but unchanged in C3H mice. Sciatic neurectomy decreased endosteal MAR in B6, but not C3H, mice.

Table 16. Effects of sciatic neurectomy on bone histomorphometric measurements at the tibial-fibular junction in C3H and B6 mice.

Mouse strain	Treatment	Medullary area (mm2)	Resorbing surface (%)	Forming surface (%)	MAR (μm/day)
C3H	Sham	0.157±0.006	0.311±0.012	0.598±0.032	--------
	Neurec	0.138±0.009*	0.308±0.017	0.692±0.017	1.38±0.07
	control	0.126±0.017*	0.472±0.049*	0.528±0.049%	1.33±0.10
	Neurec.		&		
B6	Sham	0.294±0.009@	0.208±0.018	0.673±0.044	--------
	Neurec	0.313±0.020@	0.168±0.029^	0.783±0.034	1.11±0.07^
	control	0.388±0.019*+	0.883±0.029#	0.096±0.031#	0.64±0.18+
	Neurec.	@	&@	&@	@

Neurectomy group = the neurectomized legs; neurectomy control group = the control legs of the neurectomized animals; sham group = the average of values obtained from the left and right legs from the sham operated group, as there were no differences between them. All data shown as mean±SEM (n=10).
*Different from sham surgery controls, P<0.05, #P<0.005; ^different from neurectomy-controls, P<0.05; &P<0.005; +different from C3H mice receiving the same treated, P<0.01, @P<0.001.

We did not evaluate the effects of sciatic neurectomy on total bone area at the tibial-fibular junction because we observed irregular periosteal woven bone formation in more than half of the immobilized legs. Although we have postulated that this periosteal bone formation was caused by the mice gnawing on their numb hindlimbs, we could not dismiss the possibility that the periosteal bone formation also effected endosteum. To address this possibility, we made additional measurements in ground sections, at a secondary site, i.e., in the proximal metaphysis, which was free of such irregular periosteal bone formation. Although we found strain-related differences in total bone area (1.45±0.02 mm2 for B6 sham-controls, compared to 1.07±0.02 mm2 for C3H sham-controls, P<0.001) and medullary area (0.285±0.009 mm2 for C3H sham-operated mice, compared to 0.636±0.013 mm2 for B6 sham control, P<0.001) at this proximal tibial site, we found no effects of

neurectomy on either of those two parameters. The results of our measurements of endosteal forming and resorbing surfaces at this site in the tibial metaphysis are summarized in Table 17. We found no significant effects of sciatic neurectomy on either forming or resorbing surfaces in the C3H mice; however, our studies revealed a neurectomy-dependent increase in resorbing surface length at this site in the B6 mice, as well as a neurectomy-dependent decrease in the length of forming surface in that strain.

Table 17. Effects of sciatic neurectomy on bone histomorphometric measurements at the tibial metaphysis in C3H and B6 mice.

Mouse strain (n)	Treatment	Medullary area (mm2)	Resorbing surface (%)	Forming surface (%)	MAR (μm/day)
C3H (8)	Sham	0.360±0.030	1.66±0.05	0.175±0.016	0.790±0.019
	Neurec	0.368±0.047	1.78±0.06	0.168±0.019	0.817±0.023
	control	0.439±0.038	1.58±0.079	0.210±0.018	0.758±0.033
	Neurec.				
B6	Sham	0.157±0.033	3.16±0.07@	0.040±0.009@	0.951±0.012^
	Neurec	0.158±0.038	3.20±0.09@	0.046±0.011@	0.932±0.017
	control	1.150±0.131*#	2.13±0.02*#@	0.329±0.038*#	0.610±0.056+
	Neurec.	@		@	#^

Neurectomy group = the neurectomized legs; neurectomy control group = the control legs of the neurectomized animals; sham group = the average of values obtained from the left and right legs, as there were no differences between them. All data shown as mean±SEM.
*Different from sham surgery controls, P<0.005, #different from neurectomy-controls, P<0.005; ^different from C3H mice receiving the same treated, P<0.05, @P<0.005.

In summary, sciatic neurectomy had differential effects on bone formation and resorption in the tibiae of C3H, compared to B6, mice. The left-side denervation decreased bone formation indices in the tibiae of B6 mice, but did not alter bone formation in the C3H mice. Although the immobilizing neurectomy increased bone resorption in the tibiae of both strains, the effect was greater (both in absolute and relative terms) in the B6 mice. We did not observe a systemic response (i.e., in serum ALP or OC), nor did we see a difference in ALP or osteocalcin in extracts of femora, suggesting that the skeletal effects of immobilization were localized and greatest in the most distal regions of the hindlimb skeleton. The effect of sciatic neurectomy to increase bone resorption at the tibial-fibular junction in the B6 mice (e.g., a 325% increase in percent resorbing surface, P<0.001) was consistent with effects observed in the proximal tibial metaphysis (e.g., a 722% increase in percent resorbing surface, P<0.001) and with previous reports of the effects of immobilization to increase bone resorption. In contrast, our studies showed a relatively small effect of sciatic neurectomy to increase bone resorption at the tibial-fibular junction of the C3H mice (e.g., a 51% increase in percent resorbing surface, P<0.05) and no significant effect on bone resorption in the proximal tibial metaphysis. It is interesting to speculate that these strain-associated differences in the effects of immobilization to increase bone resorption may be related to differences in the availability and/or responsiveness of osteoclast progenitor cells in the marrow of C3H and B6 mice. Further studies are required to address a parallel hypothesis concerning the differential effects of immobilization on bone formation indices in these two inbred strains of mice. The effects of sciatic neurectomy to inhibit bone formation at the tibial-fibular junction of the B6 mice (e.g., an 86% decrease in percent forming surface, P<0.001) was consistent with decreases seen in the proximal tibial metaphysis (e.g., a 36% decrease in percent forming surface, P<0.05) and with previous reports of immobilization-dependent decreases in bone formation. In contrast, our studies showed that immobilization had no such effect to inhibit bone formation in the tibiae of C3H mice. It is interesting to speculate that this

unexpected strain-associated difference may be related to differences in the availability and/or activity of osteoblast-line cells in C3H, compared to B6 mice. This information, if confirmed, is very relevant to our continued efforts in searching for gene(s) that determine peak bone mass.

B. ***Dietary calcium depletion and repletion***. To test the hypothesis that the C3H and B6 mice may differ in responses to bone resorption stimuli, we performed a preliminary study to test whether C3H and B6 mice would respond differently to challenges by dietary calcium depletion and repletion on bone resorption histomorphometric parameters. It has been well documented that dietary calcium depletion causes hypocalcemia, which leads to secondary hyperparathyroidism, subsequently resulting in increased bone resorption. Conversely, dietary calcium repletion reversed the effects, leading to a rapid reduction in bone resorption rate and an increase in bone formation.

In this preliminary study fifty mice of each strain of 4 weeks old were randomly divided into 5 groups (10 mice per group): a) baseline group, b) depletion control group, c) calcium depletion group, d) repletion control group, and e) calcium repletion group. The calcium depletion groups were fed a calcium-deficient diet containing <0.01% calcium for 14 days. The calcium repletion groups were first fed the calcium-deficient diet for 14 days, and were then re-fed a calcium-rich diet containing 0.6% calcium for an additional 14 days. The control groups were fed the calcium-containing diet throughout. The calcium depletion and their respective control groups of mice were injected with tetracycline, calcein, and tetracycline on day 0, 7, and 13, respectively, to label new bone formation. In contrast, the calcium repletion and corresponding control groups received tetracycline, calcein, and tetracycline, on day 14, 21, and 27, respectively. The baseline groups were euthanized on day 0 of the study. The calcium depletion and depletion groups were euthanized on day 14 at the end of the depletion phase; whereas the calcium repletion and their corresponding control groups were sacrificed on day 28 after the completion of the repletion phase. Blood samples were collected from each mouse for serum calcium, ALP, OC, PTH, and 1,25(OH)2D3 measurements. On the day of the euthanasia, the femora were removed from each mice for determinations of dried bone weight, bone ALP and OC contents. Ground sections of tibiae of each mouse at the tibial-fibular junction were prepared and cross-section bone histomorphometric parameters, i.e., bone area, MAR, TLS, BFR, and bone resorption rate were measured.

Table 18. Effects of calcium depletion and repletion on bone areas in C3H and B6 mice.

Strain	Treatment group (n)	Total cross-sectional area (mm2)	Medullary area (mm2)
C3H	baseline (8)	0.856±0.026	0.253±0.009
	Depletion control (6)	1.059±0.027	0.242±0.007
	Depletion (5)	0.991±0.036	0.383±0.022#
	Repletion control (5)	1.075±0.023	0.231±0.008
	Repletion (5)	1.056±0.030	0.258±0.020
B6	Baseline (5)	0.965±0.014*	0.443±0.011*
	Depletion control (6)	1.048±0.031	0.424±0.019
	Depletion (5)	1.022±0.014	0.484±0.010^
	Repletion control (5)	1.062±0.021	0.389±0.010
	Repletion (5)	1.078±0.024	0.429±0.013

Results are shown as mean±SEM. *Different from C3H mice of corresponding groups, P<0.05; #different from the depletion control group, P<0.05. ^P=0.083 when compared to its depletion control mice.

Our preliminary study indicates that two weeks of calcium depletion significantly increased the medullary area in C3H mice, a finding consistent with the contention that endosteal bone resorption in this mouse strain was elevated during dietary calcium depletion. The medullary area in B6 mice after the two weeks of calcium depletion was also slightly increased; however, the difference did not reach a statistically significant level. Upon two weeks of repletion, the differences in medullary area in either mouse strain were no longer significant. Accordingly, these findings are consistent with the previous reported effects of calcium depletion and repletion on bone resorption and formation. Consequently, these observations indicate that both mouse strains appeared to respond to the challenge of calcium depletion and repletion. As a result, these findings do not support our hypothesis that osteoclasts in C3H may be less responsive to resorption stimuli than those in B6 mice. In summary, this preliminary study of calcium depletion-repletion in C3H and B6 mice suggest that osteoclasts in these two mouse strains are responsive to physiological stimuli, such as calcium deficiency.

III. Research Aims for year 3. Our original goals for year 3 of this project was a) to continue processing bone samples from the 14 BXH RI strains plus companion B6 controls as well as any remaining B6xC3 F1 hybrid bone specimens for histomorphometric analyses of bone formation and resorption processes; b) to continue evaluate serum samples of these mouse strains and their progeny for biochemical markers for bone formation and resorption; and c) to analyze serum or bone samples of any additional groups of mice obtained from the Jackson Laboratory colonies.

However, on the basis of our progress thus far, we have revised our proposed research goals for year 3 as the following: a) we will complete any bone histomorphometric measurements that have not been finished during the first two years; b) we will focus on vertebra samples and also samples obtained from F1 progenies; c) because our recent data indicate that congenic mice are probably more suitable for genetic analyses than BXH RI strain, we will shift our emphasis to the congenic mice produced in the Jackson Laboratory; d) we will also continue to evaluate the possibility that the C3H mice and B6 mice may differ in these responsiveness to bone formation and resorption stimuli.

REFERENCES

1. Glastre, C., Braillon, P., Cochat, P., Meunier, P. J., and Delmas, P. D. Measurement of bone mineral content of the lumbar spine by DEXA in normal children: correlations with growth parameters., J Clin Endocrinol Metab. *70:* 1330-1333, 1990.
2. Theintz, G., Buchs, B., Rizzoli, R., Slosman, D., Clavien, H., Sizonenki, P. C., and Bonjour, J. P. Longitudinal monitoring of bone mass accumulation in healthy adolescents: evidence for a marked reductio after 16 years of age at the levels of lumbar spine and femoral neck in female subjects, J Clin Endocrinol Metab. *75:* 1060-1065, 1992.
3. Teegarden, D., Proulx, W. R., Martin, B. R., Zhao, J., McCabe, G. P., Lyle, R. M., Peacock, M., Slemenda, C., Johnston, C. C., and Weaver, C. M. Peak bone mass in young women., J. Bone Miner. Res. *10:* 711-715, 1995.
4. Pocock, N. A., Eisman, J. A., Hopper, J. L., Yeates, M. G., Sambrook, P. N., and Eberl, S.Genetic determinants of bone mass in adults: A twin study, J Clin Invest. *80:* 706-710, 1987.
5. Slemenda, C. W., Christian, J. C., Williams, C. J., Norton, J. A., and Johnston, C. C. J. Genetic determinants of bone mass in adult women: a reevaluation of the twin model and the potential importance of gene interaction on heritability estimates, J Bone Miner Res. *6:* 561-567, 1991.
6. Slemenda, C. W., Christian, J. C., Reed, T., Reister, T. K., Williams, C. J., and Johnston, C. C. J. Long-term bone loss in men: effects of genetic and environmental factors, Ann Intern Med. *117:* 286-291, 1992.
7. Smith, D. M., Nance, W. E., Kang, K. W., Christian, J. C., and Johnston, C. C. Genetic factors in determining bone mass, J Clin Invest. *52:* 2800-2808, 1973.
8. Hansen, M. A., Hassager, C., Jensen, S. B., and Christiansen, C. Is heritability a risk factor for postmenopausal osteoporosis, J Bone Miner Res. *9:* 1037-1043, 1992.
9. McKay, H. A., Bailey, D. A., Wilkinson, A. A., and Houston, C. S. Familial comparison of bone mineral density at the proximal femur and lumbar spine, Bone Mineral. *24:* 95-107, 1994.
10. Kelly, P. J., Hopper, J. U. L., Macaskill, G. T., Pocock, N. A., Sambrook, P. H., and Eisman, J. A. Genetic factors in bone turnover, J Clin Endocrinol Metab. *72:* 808-14, 1991.
11. Morrison, N., Yeomans, R., Kelly, P., and Eisman, J. A. Osteocalcin levels define functionally different alleles of the human vitamin D receptor, Proc Natl Acad Sci USA. *89:* 6665-6669, 1992.
12. Beamer, W. G., Donahue, L. R., Rosen, C. J., and Baylink, D. J. Genetic variability in adult bone density among inbred strains of mice, Bone. *18:*, 1996.
13. Chapman, V. M. and Nadeau, J. H. The mouse genome: an overview, Current Opinion in Genetics and Development. *2:* 406-411, 1992.
14. Foy, C., Newton, V., Wellesley, D., Harris, R., and Read, A. P. Assignment of the locus for Waardenburg syndrome type 1 to human chromosone 2q37 and possible homology to the Splotch mouse, Am J Hum Genet. *46:* 1017-1023, 1990.
15. Tassabehji, M., Read, A. P., Newton, V. E., Harris, R., Balling, R., Gruss, P., and Strachan, T. Waardenburg's syndrome patients have mutations in the human homologue of the Pax-3 paired box gene, Nature. *355:* 635-636, 1992.
16. Wright, A. F. New insights into genetic eye disease, Trends Genet. *8:* 85-91, 1992.
17. Marks, S. C. and Lane, P. W. Osteopetrosis, a new recessice skeletal mutation on chromosome 12 of the mouse, J Hered. *67:* 11-18, 1976.
18. Eicher, E. M., Southard, J. L., Scriver, C. R., and Glorieux, F. H. Hypothosphatemia: a mouse model for human familial hypophosphatemic (vitamin D-resistant) rickets, Proc Natl Acad Sci USA. *73:* 4667-4671, 1976.

19. Lewis, D. B., Liggitt, H. D., Effmann, E. L., Motley, S. T., Teitelbaum, S. L., Jepsen, K. J., Goldstein, S. A., Bonadio, J., Carpenter, J., and Perlmutter, R. M. Osteoporosis induced in mice by overproduction of interleukin 4, Proc Natl Acad Sci USA. *90:* 11618-11622, 1993.
20. Schnieke, A., Harbers, K., and Jaenisch, R. Embryonic lethal mutation in mice induced by retrovirus insertion into the α1 (I) collagen gene, Nature. *304:* 315-320, 1983.
21. Soriano, P., Montgomery, C., Geske, R., and Bradley, A. Targeted disruption of the *c-src* proto-oncogene leads to osteopetrosis in mice, Cell. *64:* 693-702, 1991.
22. Lander, E. S. and Botstein, D. Mapping mendelian factors underlying quantitative traits using RFLP linkage maps, Genetics. *121:* 185-199, 1989.
23. Chromosome committee reports, Mamm Genome. *6:* S1-S296, 1994.
24. Lander, E. S., Green, P., Abrahamson, J., Barlow, A., Daly, M. J., Lincoln, S. E., and Newburg, L. MAPMAKER: an interactive computer package for constructing primary genetic linkage maps of experimental and natural populations, Genomics. *1:* 174-181, 1987.
25. Zeng, Z.-B. Theoretical basis for separation of multiple linked gene effects in mapping quantitative trait loci, PNAS. *90:*, 1993.
26. Jansen, R. C. and Stam, P. High resolution of quantitative traits into multiple loci via interval mapping, Genetics. *136:* 1447-1455, 1994.
27. Zeng, Z.-B. Precision mappling of quantitative trait loci, Genetics. *136:* 1457-1468, 1994.
28. Jiang, C. and Aeng, Z.-B. Multiple trait analysis of genetic mapping for quantitative trait loci, Genetics. *140:* 1111-1127, 1995.
29. Lander, E. S. and Krugliak, L. Genetic dissection of complex traits: Guidelines for interpreting and reporting results. Nature Genetics 11:241-247, 1995.

DEPARTMENT OF THE ARMY
US ARMY MEDICAL RESEARCH AND MATERIEL COMMAND
504 SCOTT STREET
FORT DETRICK, MARYLAND 21702-5012

REPLY TO
ATTENTION OF:

MCMR-RMI-S (70-1y) 27 Feb 03

MEMORANDUM FOR Administrator, Defense Technical Information Center (DTIC-OCA), 8725 John J. Kingman Road, Fort Belvoir, VA 22060-6218

SUBJECT: Request Change in Distribution Statement

1. The U.S. Army Medical Research and Materiel Command has reexamined the need for the limitation assigned to the enclosed list of technical documents. Request the limited distribution statement assigned to the documents listed be changed to "Approved for public release; distribution unlimited." These documents should be released to the National Technical Information Service.

2. Point of contact for this request is Ms. Judy Pawlus at DSN 343-7322 or by e-mail at judy.pawlus@det.amedd.army.mil.

FOR THE COMMANDER:

Encl

PHYLIS M. RINEHART
Deputy Chief of Staff for
Information Management

ADB243021
ADB262474
ADB284009
ADB257455
ADB257446
ADB261351
ADB259684
ADB282142
ADB285141
ADB272522
ADB284022
ADB283904

encl